Journal of Thermal Engineering, Vol. 3, No. 3, pp. 1196-1210, July, 2017
Yildiz Technical University Press, Istanbul, Turkey

THE EFFECTS OF COOLANT PIPE GEOMETRY AND FLOW CONDITIONS ON TURBINE BLADE FILM COOLING

M. K. Akbar[1,*], B. Alsaidi[1], R. Painter[2], L. Sharpe[3], S. M. Ghiaasiaan[4]

ABSTRACT

The performance of gas turbine engines can be improved by increasing the inlet gas temperature. Turbine blades can be damaged by high gas temperature, unless additional cooling mechanisms are incorporated to maintain the blades below an acceptable temperature limit. Film cooling techniques are often used to cool the blades to avoid damages. The performance of film cooling depends on several parameters, however. In this paper past research on film cooling is reviewed and areas in need of further investigation are identified. Computational fluid dynamics (CFD) simulations are then conducted on the widely-used single-hole film cooling arrangements in which coolant jets are injected into air flows inside a straight channel before issuing onto the blades. Cooling pipe-blade configurations and flow conditions are varied and the resulting flow hydrodynamics are examined. Counter rotating vortex pairs (CRVPs) formed in the flow strongly influence the film cooling performance. Small coolant inclination angles, exit holes enlargement in span wise direction, higher injected fluid density, and higher injected-ambient fluid velocity ratios are all found to maintain the CRVPs away from each other and close to wall - both of which promote cooling. Pipe curvature can be used for enhancing cooling by exploiting the centrifugal force effect.

Keywords: *Numerical Study, Gas Turbine Blade, Counter Rotating Vortex Pairs, Recirculation Zone, Flow Hydrodynamics, Film Cooling Effectiveness*

INTRODUCTION

High gas inlet temperature is one of the major parameters that can increase the power output and cycle efficiency of gas turbine engines. The highest feasible gas inlet temperature is limited by the vulnerability of the turbine blades, however, which need to remain at temperatures below their limit of tolerance. However, with careful design of the blades and flow passages as well as utilization of a blade cooling arrangement the temperature of the inlet hot gas may even reach above the blade melting temperatures. Among the popular blade cooling arrangements are the film cooling techniques. The cooling performance is then governed by complex flow characteristics formed by the coolant stream effusing into the boundary layer on the surface of the gas turbine blades. Among the most unfavorable complex structures is a counter rotating vortex pair (CRVP). Significant research aimed at understanding the flow characteristics and improving the efficiency of film cooling techniques has been reported. However, as will be shown below, some important aspects of the film cooling technique, with respect to parametric dependencies and their underlying causes, are not well understood**.**

REVIEW OF PAST RESEARCH

Cylindrical film cooling holes are the most economical to manufacture and traditional film cooling research is heavily focused on simple cylindrical hole geometries (e.g, [1-5]). The average film cooling effectiveness is reported to depend on the mass flux ratio (MR), although this dependence is not monotonic. The effectiveness rises as the MR increases first, until it reaches a peak. Further increasing the mass flux ratio will then lead to a reduction in the effectiveness. The threshold MR value was found by Baldauf et al. [4] to be about 0.85. However, Thole et al. [6] found that coolant jet separation is primarily a function of momentum flux ratio (IR), not MR. The flow is fully attached when the IR is less than 0.4. The flow initially detaches, but reattaches if the IR value is between 0.4 and 0.8. The flow is fully detached if the IR is higher than 0.8. Jessen et al. [7] reported that a higher velocity ratio (VR) enlarges the size of the recirculation region leading to a more pronounced

This paper was recommended for publication in revised form by Regional Editor Mohammed Sajjad Mayeed
[1]Mechanical and Manufacturing Engineering Department, Tennessee State University, Nashville, Tennessee, USA
[2]Civil and Architectural Engineering Department, Tennessee State University, Nashville, Tennessee, USA
[3]Massie Chair of Excellence Dean of Life and Physical Sciences Tennessee State University, Nashville, Tennessee, USA
[4]W. Woodruff School of Mechanical Engineering Georgia Institute of Technology, Atlanta, Georgia, USA
**E-mail address: makbar@tnstate.edu*
Manuscript Received 24 October 2016, Accepted 8 December 2016

entrainment of crossflow fluid into the wake of the jet. Velocity effects dominate the flow field in the vicinity of the jet hole.

The blowing or inclination angle (θ) plays an important role in film cooling. When the blowing angle is small, the jet is prone to cover the cooling surface effectively. However, a very small blowing angle may limit the coverage region [1-4]. An increase in the injection angle results in a slight decrease in the film cooling effectiveness for a low blowing ratio of 0.5. However, the effectiveness was observed to decrease significantly for the high blowing ratio of 1 [8]. The cooling jet diffuses significantly at higher injection angles. Despite the known advantage of low inclination angles, the backward injection (i.e., inclination angle more than 90°) is found to improve the film cooling performance on flat surface at both laboratory and gas turbine operating conditions with blowing ratio more than 0.75 [9].

Lowering the density ratio (DR) for coolant jets tends to cause the jets to separate earlier. Consequently the maximum film effectiveness is reduced by lowering the density ratio of the coolant jets. For example, Pedersen et al. [2], Sinha et al. [3], and Baldauf et al. [4] found that the maximum laterally averaged film effectiveness was about 20% higher for coolant DR ≈ 2 compared to DR ≈ 1.2 near the hole (x/d <20) but was essentially the same farther downstream. The DR alone cannot determine the effectiveness and the primary factor influencing the film effectiveness is claimed to be the IR instead. Nevertheless, Jessen et al. [7] found that the lateral spreading of the coolant downstream, which is crucial for the cooling efficiency, is strongly increased by increasing the DR.

It is established that the interaction between the main stream flow and the coolant flow generates a very complex flow structure (e.g., [10-17]). It is found that a counter rotating vortex pair (CRVP) may form at the jet mixing locations which affects the jet liftoff and is thus one of the major contributors to reduced film cooling performance. The CRVP mechanism increases the aerodynamic mixing of the jet with the crossflow and causes a delay in the reattachment of the cooling jet to the blade's surface due to the jet lift-off effects. Unfortunately, most of the earliest film cooling studies do not discuss the generation and transport of CRVP comprehensively.

The shape of the jet holes is known to influence CRVP and cooling effectiveness [5], although no single shaping of film holes can provide an optimal hydrodynamics. For example, the circular exit hole is found to improve the jet adhesion to the wall surface and reduces the jet lift-off effect [18]. However, Takahashi et al. [14] found that rectangular holes achieved higher film cooling effectiveness compare with circular holes due to greater spreading of the film cooling jet over the blade surface. It was noticed that the jet exit cross-section aspect ratio (defined as the ratio between the spanwise and streamwise dimensions) is an important parameter, but it is significant only in the near field and its effect diminishes in the far field [13]. In the case of a low aspect ratio, two counter-rotating pairs of vortices are initially formed at the sides of the jet, with the weaker pair subsequently entrained by the stronger pair further downstream. For high-aspect-ratio jets, only one CRVP is formed throughout the jet column, but the shear layer develops additional folds along the windward side of the jet.

The mechanism of CRVP changes altogether in the presence of secondary blowing holes. For example, a high film cooling effectiveness is achieved at higher blowing in the presence of discrete sister holes [12], which augments the coolant attachment to the plate surface and reduces the aerodynamic losses by weakening CRVP. A vortex generator system can be used to increase cooling by creating anti-counter rotating vortex pairs (ACRVP). Rigby and Heidmann [16] placed a delta shaped object downstream of the injection hole in their model. The coolant pushed towards the wall surface and spread out along the wall as a result of the ACRVP. A considerable reduction in the strength of the CRVP when using the compound angled holes has been observed in the experimental work of Aga et al. [15]. For the high blowing ratio of 3, no jet lift-off is reported. Moreover, the coolant is spread more in the spanwise direction for the compound angled holes as compared with the streamwise injection. All in all, it is evident that the primary and/or secondary hole configurations can significantly alter the CRVP and film cooling effectiveness. Therefore, it is not surprising at all that Bunker [5] predicted, with a better manufacturability, unconventional hole configurations which are more effective with less air will become more viable.

In the present study, numerical simulations have been conducted to understand the flow hydrodynamics of various single-hole film cooling configurations. The inclination angle, pipe curvature, exit hole size and shape, fluid density and velocity ratios are varied parametrically to elucidate their influence on the hydrodynamics and film cooling effectiveness. The purpose of re-visiting this classical problem is to investigate the phenomenology of the CRVPs and their influence on the film cooling. The movement of the CRVPs is tracked and the effect of such motion on the film effectiveness is examined.

MODELING APPROACH AND VERIFICATION

The ANSYS FLUENT R16.1 [19] is used as the simulation tool in the present study. The pressure-based, steady state, and incompressible-ideal gas solver with energy equation are used to solve the governing equations. The density of the fluid is calculated assuming ideal gas law based on the operating pressure, which is set to atmospheric pressure. Other properties are calculated using the Kinetic Theory - Sutherland's Law option of FLUENT, which calculates those properties based on a formula proposed by Sutherland [20]. It should be noted that the flow Mach number of the cases run here are significantly lower than 0.3.

Johnson et al. [21], Zhang and Hassan [10], and Khajehhasani [12] performed CFD simulations with various Reynolds Average Navier-Stokes RANS) turbulence models. Based on previous researchers' recommendations, the realizable k–ε turbulence closure model is used with enhanced wall treatment option in the present study. The relevant conservation equations are presented and thoroughly explained in ANSYS FLUENT Theory Guide [19] and numerous other publications (e.g., [22-25]), and hence will not be repeated here.

Discretization is accomplished with the second-order upwind scheme for all spatial terms in conservation equations. The SIMPLE segregated algorithm is used to deal with pressure-velocity coupling. The gradient term is calculated using least squares cell based option. For a given iteration, the three momentum equations are solved sequentially, followed by a pressure-correction continuity equation. After the fluxes are updated based on these new solutions, scalar values such as temperature and turbulence quantities are calculated. Convergence is dictated by residual criteria set below 10–6 for all equations. The solution convergence process is controlled by under-relaxation factors for each of the equations. The momentum under-relaxation factor is found to be the most important one to avoid any divergence, and it is set to 0.5.

Based on an extensive literature survey, the experimental and simulation studies of Jessen et al. [7] of single-hole cooling is chosen as the benchmark for verification. They investigated the turbulent flow structure and vortex dynamics of a jet-in-a-cross flow problem that is directly related to gas turbine blade film cooling. Jessen et al. [7] experimentally studied the problem using particle-image velocimetry (PIV) technique, as well as numerically using the Large Eddy Simulation (LES) turbulence model. A cooling jet emanating from a pipe interacted with a turbulent flat plate boundary layer at a Reynolds number (Re) of 400,000. A case with the streamwise inclination of the coolant jet of 30°, velocity ratio VR = 0.28, and density ratio DR = 1.53 is used as the benchmark. Isothermal jets of air and CO2 are injected separately into a boundary layer to examine the effects of the velocity and density ratio between coolant and mainstream on the mixing behavior and consequently, the cooling effectiveness.

The mesh is created using the Design Modeler tool of ANSYS FLUENT R16.1. Highly refined mesh is generated next to the walls. The total cell number is 13.5 million. Uniform velocity profiles are used at the inlet boundaries. At the outlet, a zero gauge pressure condition is used. Both fluid temperatures are set to 298 K. Both boundaries in the span (z) directions have symmetric boundary conditions.

Streamwise velocity profiles in the spanwise symmetry plane (z/D = 0) at different streamwise locations (x/D = 0.5, 1, 1.5, 2, 3 and 6) are shown in Figure 1, where the corresponding experimental data and simulation results of Jessen et al. [7] are also shown. The comparison, in general, is good. The profiles at location x/D = 0.5 show smaller streamwise velocity near the hole since the jet is moving upward with an injection angle of 30°. At x/D = 1 the boundary layer is pushed upward and clearly separates somewhere near x/D = 1.5. This is the location where the CRVP is formed as a result of the shear between the jet and the mainstream flow. Carbon dioxide lifting off the wall as low density air from the mainstream is entrained between the wall and the jet due to the existence of vortex. This is the phenomenon that results in the reduction of cooling effectiveness in the downstream flow. Due to strong mainstream flow the boundary layer reattaches downstream, as can be seen at x/D = 2. The velocity profiles at x/ D = 3 and x/D = 6 still depict the influence of the coolant jet. However, the influence vanishes further downstream.

Present simulation matches better than the simulation of Jessen et al. [7] with their experimental data near the hole exit. However, in downstream locations simulation of Jesses et al. performs better. One simple explanation is every turbulence model has its own advantages and disadvantages. The k–ε turbulence model is very robust and its convergence is great, but it is less accurate in areas with adverse pressure gradient, which is the case in downstream locations of the present problem. On the other hand, LES model used by Jessen et al. is generally more accurate, but computationally much expensive. Considering its computational cost effectiveness, the realizable k-ε turbulence model which is used in the present study consistently produced reasonable results when

compared with the Particle Image Velocimetry experimental data and Large Eddy Simulation results of Jessen et al. [7] and the experimental data of Sinha et al. [3]. Those are not shown for brevity.

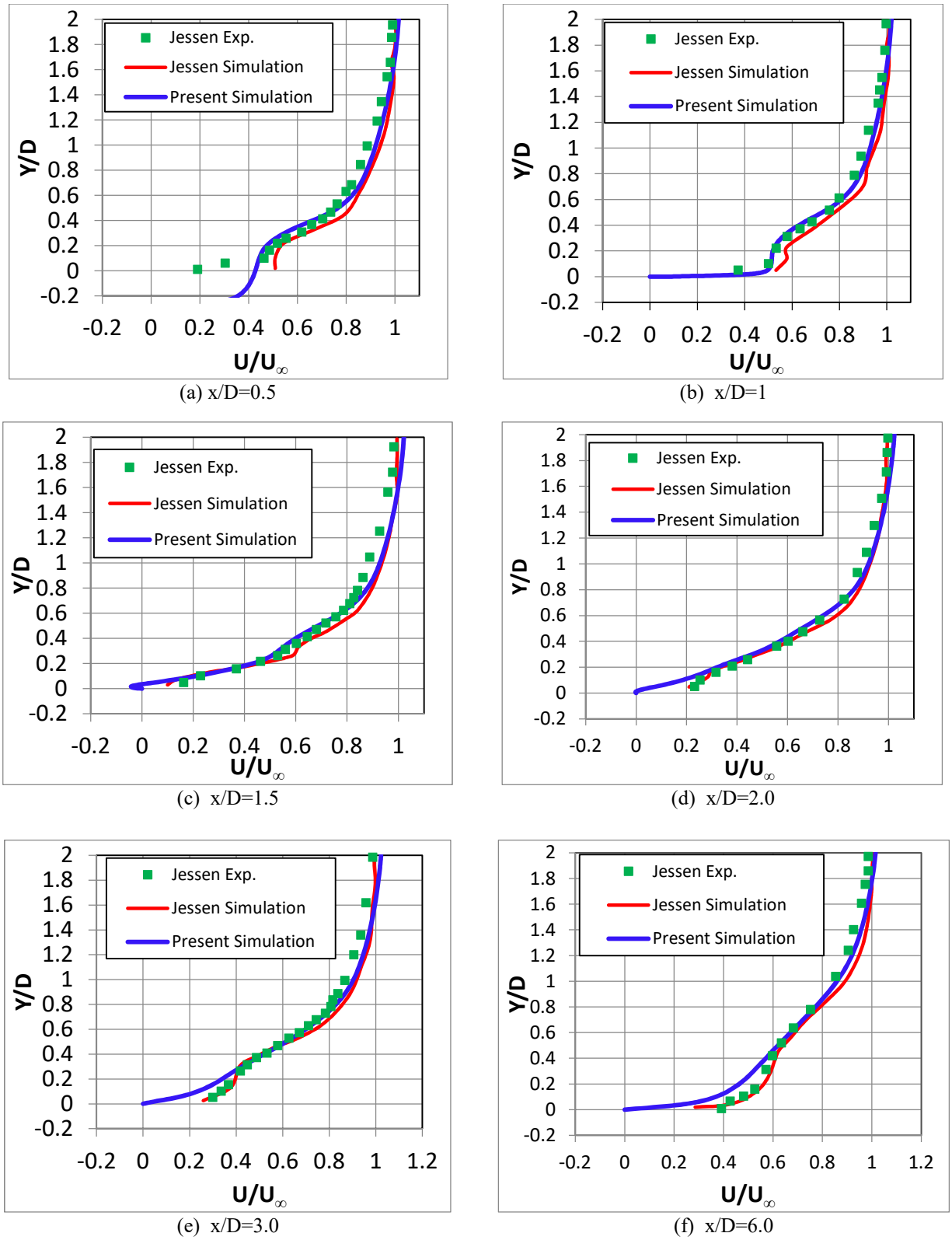

Figure 1. Comparison of present streamwise velocity profiles with those of Jessen et al. [7] at z/D = 0.0 at different streamwise locations

Table 1. Base model geometric configuration (refer to Figure 2)

Parameter	Value
X	550 mm
X_1	400 mm
Y	200 mm
Z	30 mm
D	10 mm
L	240 mm

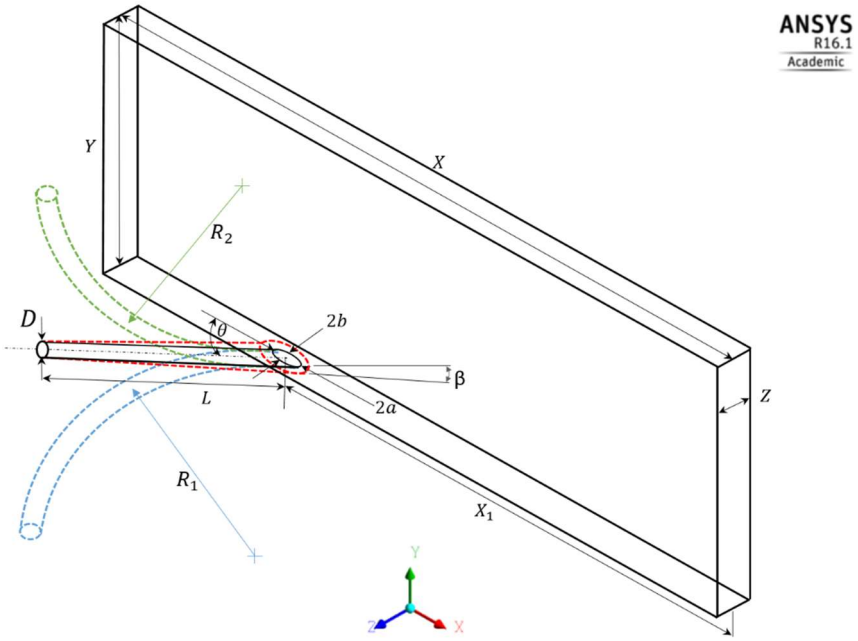

Figure 2. Geometry of the model used for numerical experiment of the coolant pipe configuration

Based on a literature survey, a set of coolant geometric features, such as pipe inclination angle, exit hole size and shape, pipe curvature, fluid density ratio, and velocity ratio are expected to influence the gas turbine film cooling effectiveness. Parametric simulations are performed to assess the movement of CRVP and their influence on film effectiveness. The dimension of the base model is summarized in Table 1. The base geometry of the simulation domain is shown in Figure 2 in solid black color. Variations of the model geometry are displayed in dotted colored lines, and detail dimensions are presented later in the parametric study section. Note that the origin of the global coordinate system is located at the center of the coolant jet exit (i.e., at the intersection of the channel and coolant pipe axis). The coolant and channel dimensions are similar to that of Jessen et al. [7] study, the benchmark problem for the present investigation.

A detailed mesh independent study was performed on the straight coolant pipe with 25° inclination angle (θ). The mesh displayed in Figure 3, which will be referred to as the base mesh has around 8×10^5 cells, and was found to be sufficient for generating mesh-independent results.

MODEL RUN CONDITIONS AND PARAMETRICS

Table 2 lists all the parametric cases that are studied. For all cases, the coolant pipe inlet is kept circular with a diameter of 10 mm. Air is used as both mainstream and coolant fluid. For most cases, uniform velocities of 8.61 m/s and 2.41 m/s are used at the mainstream inlet and coolant inlet, respectively. Temperatures of 520 (K) and 297.15 (K) are used at the mainstream inlet and coolant inlet, respectively. The turbulent intensity is set to 5% and turbulent viscosity ratio is set to 10 in all boundaries for all cases. Based on these velocity and temperature boundary conditions, most cases have the following default characteristics: velocity ratio (VR) = 0.28, density ratio (DR) = 1.76, mass flux ratio (MR) = 0.49, and momentum flux ratio (IR) = 0.14. Some of the cases have DR.

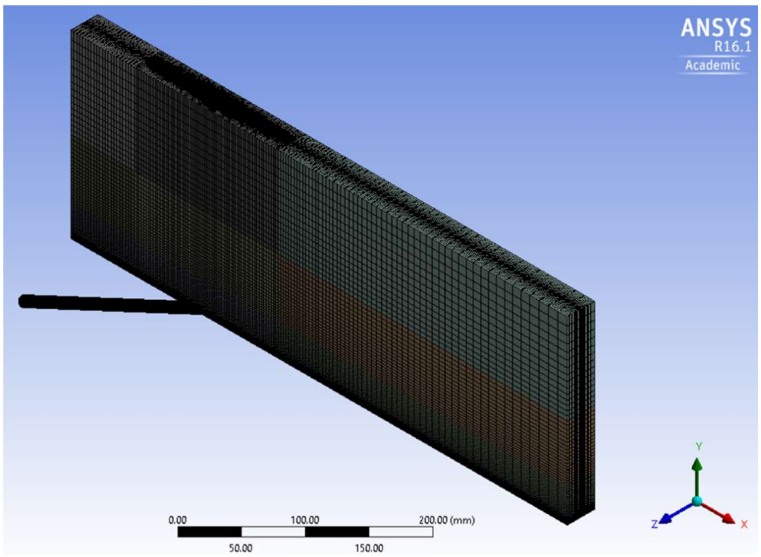

(a)

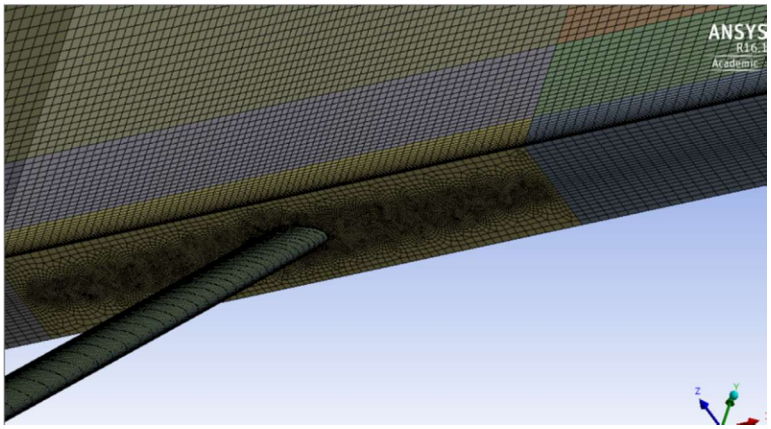

(b)

Figure 3. Mesh 4, the base model used for the parametric study (a) whole domain, (b) zoomed view at the intersection

and VR values different than default values. Some of the pipes are not straight, and have finite radius of curvatures. The comments column of Table 2 provides with some additional information to differentiate cases from each other.

RESULTS AND DISCUSSION

The average film cooling effectiveness ($\bar{\varepsilon}$), is calculated from:

$$\bar{\varepsilon} = \frac{1}{(2z)(2x)} \int_{-Z}^{Z} \int_{-X}^{X} \left(\frac{T_\infty - T(x,z)}{T_\infty - T_w} \right) dx\, dz \tag{1}$$

where 2X and 2Z represent, respectively, the streamwise and spanwise widths of the area of interest.

The average film cooling effectiveness for all parametric cases are reported on Table 2. A detail discussion is presented below.

Pipe Inclination Angle

From Table 2, it is observed that a smaller inclination angle resulted in a higher effectiveness. A similar finding for similar mass flux ratio cases is reported by previous researchers as well, such as Kohli and Bogard [8]. Li et al. [9] obtained backward jets to work better than forward jets with mass flux ratio (MR) 2.0. The present MR is 0.49, and forward jets are found to be more effective. A complex hydrodynamic pattern resulted from the mixing of two streams. Figure 4 shows the velocity contours and vectors at the coolant exit. The vector plots indicate that a lowering the coolant jet inclination angle results in a lower angle between the coolant and mainstream air. This reduces the coolant jet penetration into the boundary layer. From recirculation plots (not

shown for brevity), the boundary layer separation is found to be more visible and starts at a location closer to the hole for jets with larger inclination angles. The cross flow (Case 3) or opposing flow (Case 4) streams cause the flow to separate at the leading edge of the flow intersection. This, in turn, narrows the effective coolant jet area and increases local jet velocity and forces the coolant stream to move away from the wall. The turbulent kinetic energy increases as the inclination angle increases, which reduces the film cooling effectiveness.

Table 2. Parametric Design of Simulation (refer to Figure 2)

Case #	θ (°)	β (°)	2a/D	2b/D	R_1/D	R_2/D	DR	VR	Ave. Film Effectiveness ($\bar{\varepsilon}$)	Comments
Effect of Inclination Angles (θ)										
1	25°	0	2.37 (Auto)	1 (Auto)	∞`	∞	1.76	0.28	0.109	-
2	45°	0	1.41 (Auto)	1 (Auto)	∞	∞	1.76	0.28	0.106	-
3	90°	0	1 (Auto)	1 (Auto)	∞	∞	1.76	0.28	0.099	-
4	135°	0	1.41 (Auto)	1 (Auto)	∞	∞	1.76	0.28	0.095	-
Effect of Hole Exit Size and Shape										
5	25°	1	4.36 (Auto)	1.84 (Auto)	∞	∞	1.76	0.28	0.122	Conical pipe; elliptic exit
6	25°	-	1.54	1.54	∞	∞	1.76	0.28	0.124	Circular exit
7	25°	-	1.0	2.37	∞	∞	1.76	0.28	0.148	Elliptic exit, but rotated 90° in y-axis
Effect of Coolant Pipe Curvature										
8	25°	0	2.37 (Auto)	1.0 (Auto)	20	-	1.76	0.28	0.108	Curved pipe
9	25°	0	2.37 (Auto)	1.0 (Auto)	-	20	1.76	0.28	0.111	Reverse curved pipe, rotated 180° on xy-plane
Effect of Fluid Density Ratio (DR)										
10	25°	0	2.37 (Auto)	1.0 (Auto)	∞	∞	1.26	0.28	0.096	Mainstream & coolant at 372.4K & 297.15K
11	25°	0	2.37 (Auto)	1.0 (Auto)	∞	∞	2.27	0.28	0.123	Mainstream & coolant at 668.6K & 297.15K
Effect of Fluid Velocity Ratio (VR)										
12	25°	0	2.37 (Auto)	1.0 (Auto)	∞	∞	1.76	0.36	0.126	Mainstream & coolant at 8.61 m/s & 3.1 m/s
13	25°	0	2.37 (Auto)	1.0 (Auto)	∞	∞	1.76	0.54	0.139	Mainstream & coolant at 8.61 m/s & 4.65 m/s
Optimum Parameters										
14	25°	-	1.0	2.37	-	20	1.76	0.28	0.150	Reverse curved pipe
15	25°	-	1.0	2.37	-	20	2.27	0.28	0.172	Reverse curved pipe; mainstream at 668.6K
16	25°	-	1.0	2.37	-	20	1.76	0.36	0.179	Reverse curved pipe; coolant at 3.1 m/s

("Auto" means this dimension of the coolant pipe exit is a free variable. It is determined from the constraints placed at the inlet of the pipe)

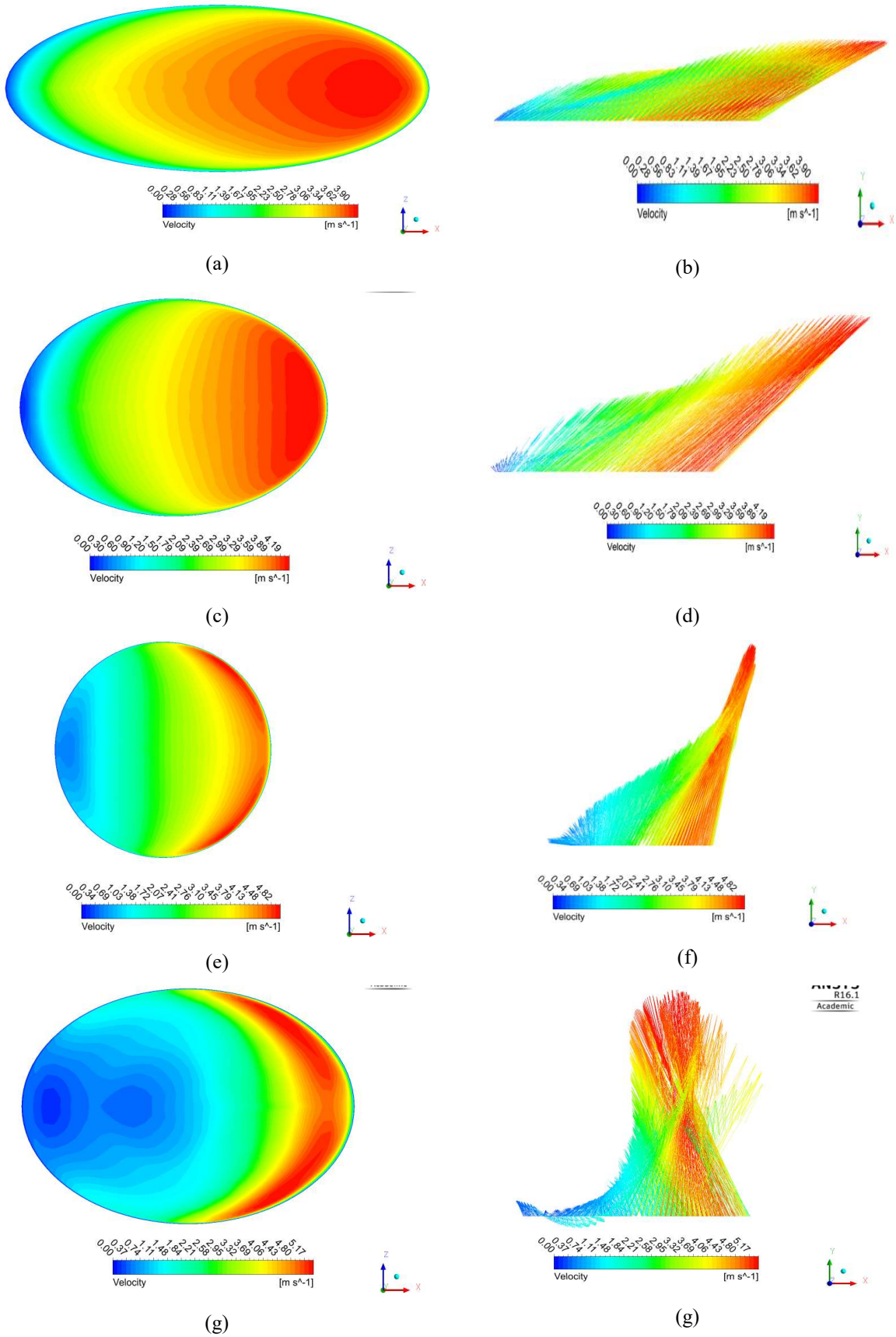

Figure 4. Velocity contours and vectors at the pipe exit hole (a)-(b) Case 1, (c)-(d) Case 2, (e)-(f) Case 3, and (g)-(h) Case 4. The filled contour plots on the left represent the top views, and the vector arrow plots on the right represent the front views of the exit hole. The shape of the hole is automatically determined based on the intersection of the pipe and mainstream channel

Perhaps the most important hydrodynamic aspect is the formation of two counter rotating vortices (CRVPs) that develop on the two span sides downstream of the holes [10, 12]. Figure 5 shows the streamline patterns of CRVP on yz-plane at x/D=1.0. Evidently, cases with larger inclination angles display larger and stronger CRVP patterns. Interesting CRVP pattern changes are noticed along the flow direction. Figure 6 displays the spanwise (z/D) and vertical (y/D) locations of one of the vortices at several x/D locations. The analysis of the streamlines shows that for smaller inclination angle cases the vortex pairs are smaller, stay close to the wall, and away from each other. With increasing the inclination angles, the vortices become larger, move higher up from the wall, and come closer to each other – all of which reduce the film cooling effectiveness. For all cases the vortices move towards the centerline first and then move away from it. For smaller inclination angle cases, this departure occurs earlier than the larger ones, which helps to increase the film cooling effectiveness.

Pipe Exit Shape and Size

A larger exit hole generally increases the effectiveness. Larger exit hole helps by reducing the jet velocity and by affecting a larger area of the mainstream flow to spread the coolant on the wall. When compared with Case 1, Case 5 improves the effectiveness, while Case 6 with a circular shape exit hole has even a better film effectiveness. The best effectiveness among these three cases is achieved by Case 7 that has an elliptic hole with larger axis in the z-direction. The recirculation plots show that Cases 5 and 7 do not have any flow separation at all. Case 7 has the lowest flow mixing, which helps keep the coolant gas near the wall.

Figure 7 displays the spanwise and vertical locations of the vortices at different x/D locations. For holes with larger exit span dimensions, the CRVPs are already far away from each other, which allows the cooling jet to stay close to the wall surface. Although the vortices for Case 5 start far from each other, later they move closer, as well as up from wall – causing Case 5 to have an inferior film cooling effectiveness than those of Case 6 and 7. We may observe, therefore, that a large exit hole spanwise dimension improves the performance, whereas the improvement caused by larger size in flow direction is insignificant.

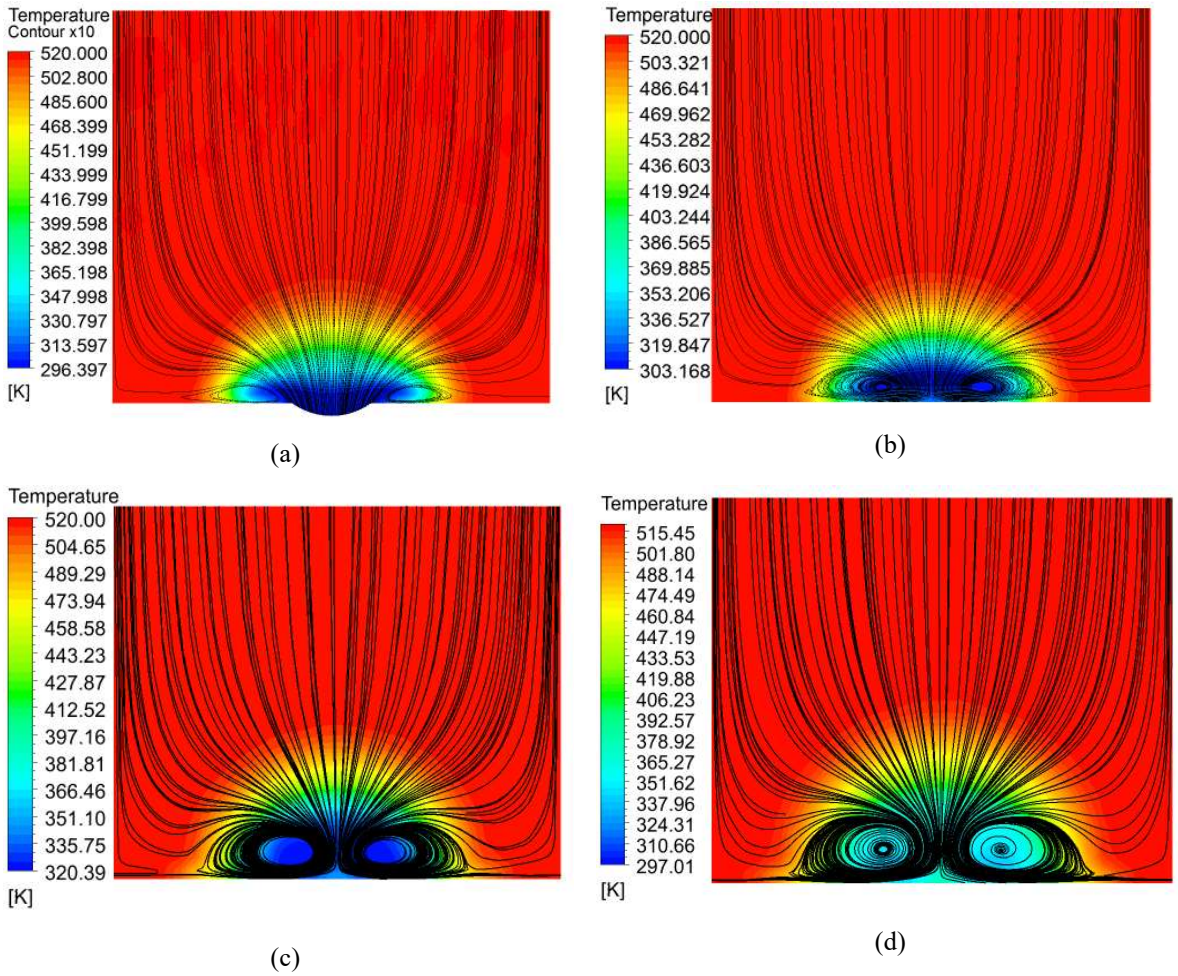

Figure 5. Counter rotating vortex pair on yz-plane at x/D=1.0 (a) Case 1, (b) Case 2, (c) Case 3, and (d) Case 4

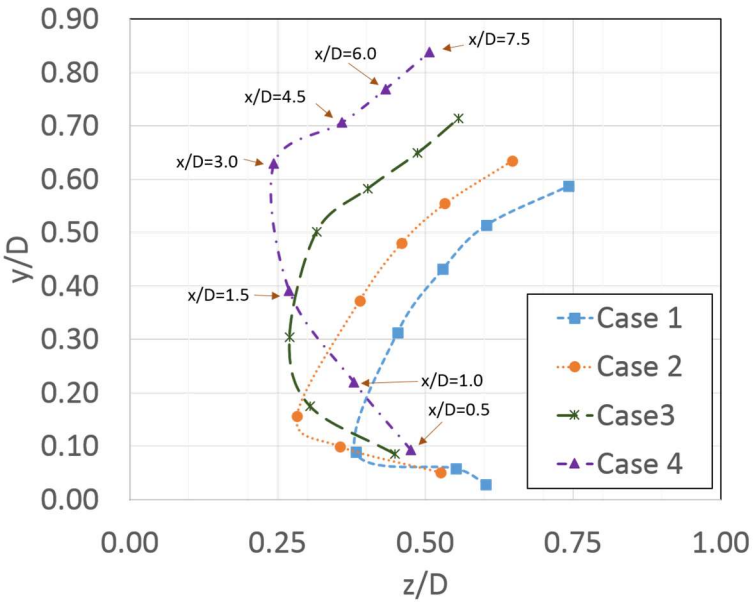

Figure 6. Counter rotating vortex pair locations on yz-plane at x/D = 7.5, 6.0, 4.5, 3.0, 1.5, 1.0, 0.5, and 0.0 sections (from top to bottom) for Case 1-4. Note: locations of only one vortex of a pair is shown. For each case, symbols from top to bottom represent data in decreasing x/D order. Some plots miss symbols at the bottom, which means CRVP have not formed yet at those x/D locations

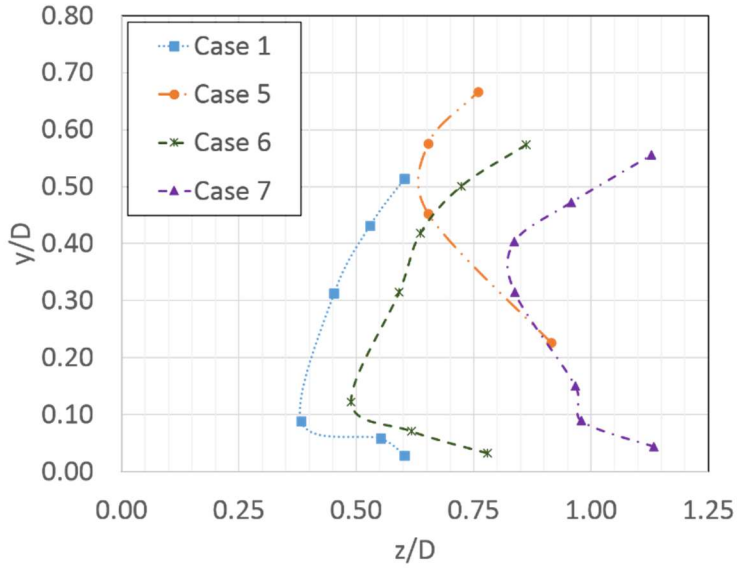

Figure 7. Counter rotating vortex pair locations on yz-plane at x/D = 7.5, 6.0, 4.5, 3.0, 1.5, 1.0, 0.5, and 0.0 sections (top to bottom) for Case 1, 5-7. Note: locations of only one vortex of a pair is shown. For each case, symbols from top to bottom represent data in decreasing x/D order. Some plots miss symbols at the bottom, which means CRVP have not formed yet at those x/D locations

Pipe Curvature

The simulation results in Table 2 indicate that the curvature of Case 8 decreases the film cooling effectiveness, while the reversed curvature of Case 9 improves the cooling effectiveness. Further analysis showed that the reversed curvature tends to increase the film cooling effectiveness away from centerline at larger z/D locations. Depending on the curvature, the exiting fluid may be far from (Case 8) or close to (Case 9) the trailing edge of the hole, as can be concluded from Figure 8. These phenomena are due to the inertia of the fluid (the centrifugal effect). Figure 9 shows the formation, location and path of CRVPs. Overall, the reversed curvature increases film cooling effectiveness.

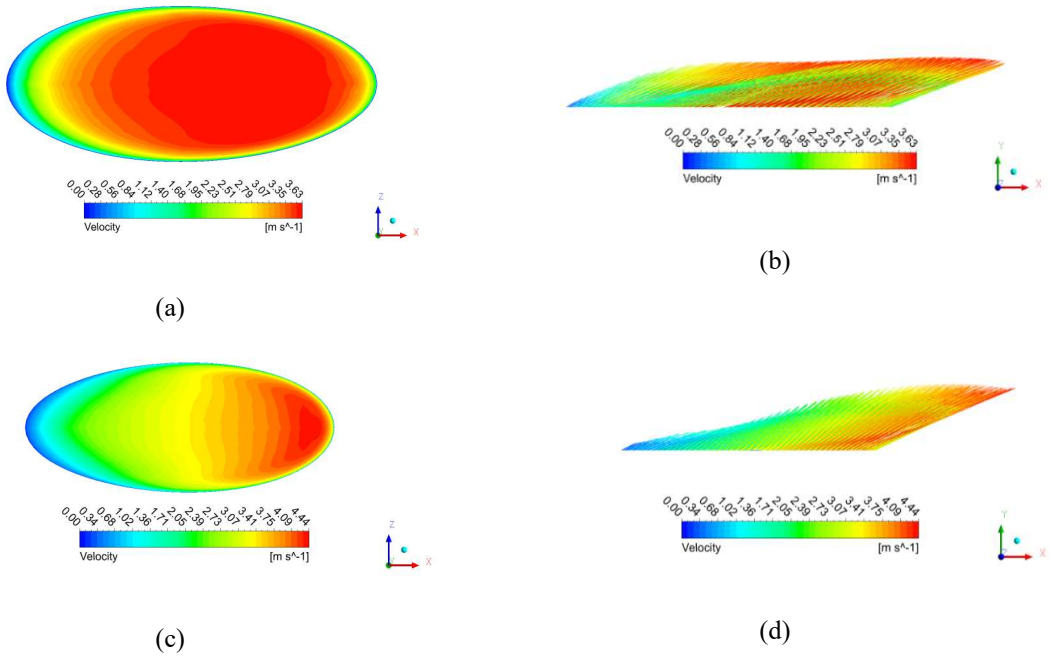

Figure 8. Velocity contours and vectors at the pipe exit hole (a)-(b) Case 8, (c)-(d) Case 9.

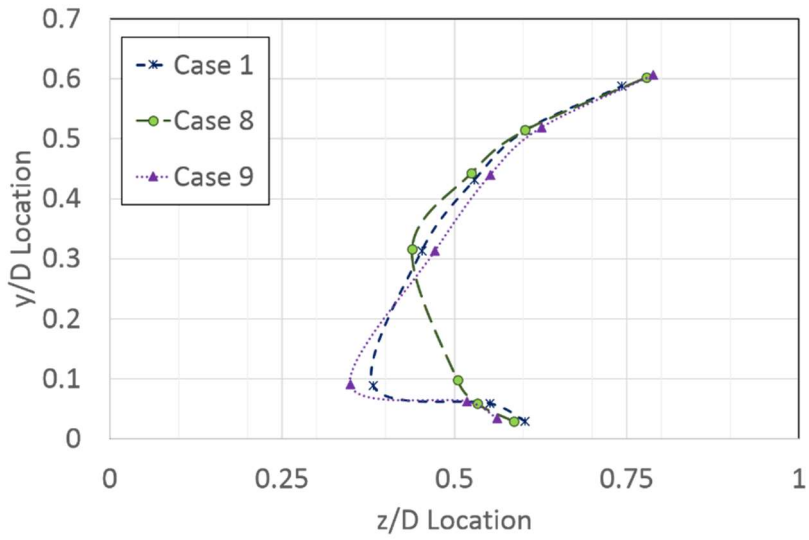

Figure 9. Counter rotating vortex pair locations on yz-plane at x/D = 7.5, 6.0, 4.5, 3.0, 1.5, 1.0, 0.5, and 0.0 sections (top to bottom) for Case 1, 8-9. Note: for each case symbols from top to bottom represent data at decreased x/D locations. Some plots miss symbols at the bottom, which means CRVP have not formed yet

Fluid Density Ratio

The parametric results in Table 2 suggest that higher coolant density, within the scope of the present study, monotonically increases the average film cooling effectiveness; an observation also supported by earlier studies. The average film cooling effectiveness increases by about 12% for each 0.5 increment of DR, which is consistent with previous studies [2-4]. Note that for a low DR case, the density of mainstream fluid is (still less, but) comparable to that of coolant fluid. The high momentum of incoming mainstream fluid presses to constrict the ensuing coolant jet, and this constriction effect is more pronounced in lower DR cases. The jet maximum velocity is higher for those lower DR cases, and hence the jet penetrates deeper into the mainstream boundary layer leading to decreased film cooling effectiveness. Higher density ratio cases keep the CRVP vortices away from each other, as can be seen in Figure 10. This separation in between the vortices promotes the film cooling effectiveness.

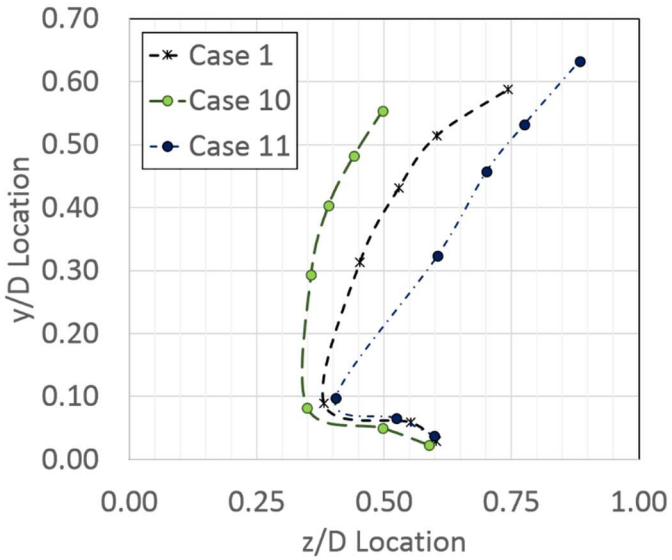

Figure 10. Counter rotating vortex pair locations on yz-plane at x/D = 7.5, 6.0, 4.5, 3.0, 1.5, 1.0, 0.5, and 0.0 sections (top to bottom) for Case 1, 10-11. Note: locations of only one vortex of a pair is shown. For each case, symbols from top to bottom represent data in decreasing x/D order. Some plots miss symbols at the bottom, which means CRVP have not formed yet at those x/D locations

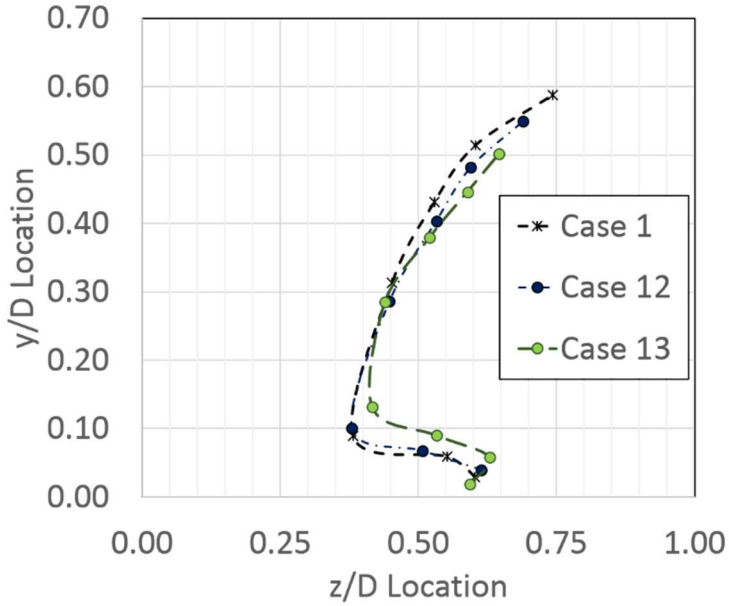

Figure 11. Counter rotating vortex pair locations on yz-plane at x/D = 7.5, 6.0, 4.5, 3.0, 1.5, 1.0, 0.5, and 0.0 sections (top to bottom) for Case 1, 12-13. Note: locations of only one vortex of a pair is shown. For each case, symbols from top to bottom represent data in decreasing x/D order. Some plots miss symbols at the bottom, which means CRVP have not formed yet at those x/D locations

Fluid Velocity Ratio

Our parametric simulation suggest that that the velocity ratio (VR) influences film cooling effectiveness. Note that if the density ratio remains the same, an increase in VR will increase mass and momentum flux ratios as well. Thole et al [6] found that for the centerline cooling jet exiting with 35° inclination angle, the average effectiveness increases with increasing MR up to an MR value of 0.8, beyond which the trend reverses. Within the scope of the present study with a jet inclination angle of 25°, however, the film cooling effectiveness increases monotonically up to an MR value of 0.95. The flow separation is known to depend heavily on momentum flux. A higher velocity ratio causes a reduction of film cooling effectiveness near the jet exit, but the trend reverses further downstream. On the other hand, a lower VR provides a higher effectiveness near the hole, but it does not carry the coolant far downstream. Figure 11 shows that CRVPs created by higher VR cases have a tendency to stay near the wall at a given streamwise location. The higher momentum associated with higher VR pushes the coolant far

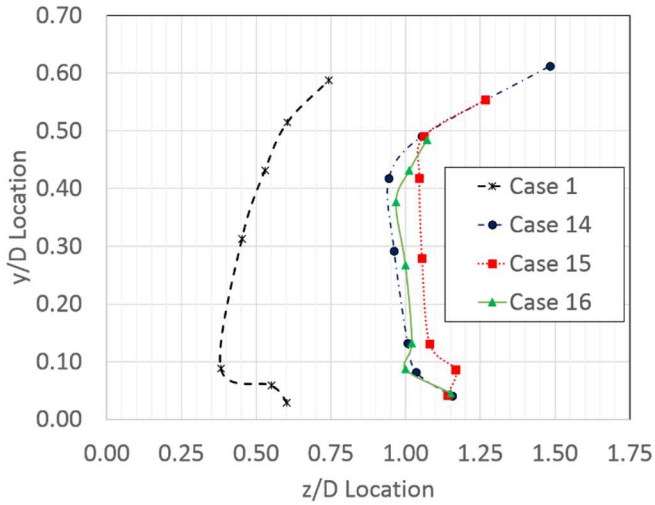

Figure 12. Counter rotating vortex pair locations on yz-plane at x/D = 7.5, 6.0, 4.5, 3.0, 1.5, 1.0, 0.5, and 0.0 sections (top to bottom) for Case 1, 14-16. Note: locations of only one vortex of a pair is shown. For each case, symbols from top to bottom represent data in decreasing x/D order. Some plots miss symbols at the bottom, which means CRVP have not formed yet at those x/D locations

downstream before the vortices can move upward. A higher VR appears to keep the vortices farther away from each other as well, although by a relatively small margin.

Optimum Combinations

In light of the aforementioned observations, one may conclude that a small inclination angle of the coolant pipe, an exit hole enlarged in the spanwise direction (z-direction in Figure 2), a high coolant density, a moderately high coolant velocity, and a reversed curvature of coolant pipe all promote film cooling effectiveness. Accordingly, in Table 2 Cases 14 through 16, all achieve increased film cooling effectiveness. This significant improvement is associated with the combined effect of reversed curvature, higher DR and VR values. Figure 12 displays the spanwise and vertical locations of the vortices at different x/D locations. All the optimal cases have CRVP that are well separated from each other, which allows cooling fluid in-between to stay near the wall surface. At a given x/D location, higher VR and DR keep the vortices close to the wall, which promotes film cooling effectiveness.

CONCLUDING REMARKS

A detailed numerical investigation of single-hole coolant pipe geometric configurations and flow conditions was conducted. It is a re-visit of a classical problem with the objectives of understanding the flow hydrodynamics of, and finding a method for improving the effectiveness of, film cooling. A set of parametric study was performed with ranges of density, velocity, mass flux, and momentum flux ratios from 1.26 to 2.27, 0.28 to 0.54, 0.35 to 0.95, and 0.10 to 0.51, respectively. The overall findings of the study are in agreement with previous studies.

The coolant jets with smaller inclination angles were more effective for film cooling. Small inclination angles cause the resultant velocity of the mainstream and coolant to stay close to the channel wall, which shrinks the flow recirculation zone downstream the jet. A small inclination angle also ensures that the counter rotating vortex pair quickly move away outward in the spanwise direction.

A circular shaped exit jet is more effective in cooling than an elliptical shaped exit jet emanating from traditional cylindrical pipes. However, turned around elliptical exit holes with larger spanwise dimensions offer a significantly better film cooling effectiveness by reducing or eliminating the recirculation zone, and keeping the counter rotating vortex pairs far apart from each other and low close to the wall. A higher coolant density positively impacts the film cooling effectiveness by keeping the vortices away from each other. On the other hand, higher velocity ratios keep the vortices near the wall. The impact of pipe reversed curvature on film cooling effectiveness is also significant, especially for the cases with high velocity and density ratios. The reversed curvature facilitates keeping the flow close to the trailing edge of the hole, which promotes film cooling effectiveness. Most of the results are well supported by previous studies. However, the effects of pipe reversed curvature on film cooling effectiveness were not studied before. Therefore, more studies and experiments are needed before such configurations can be implemented in practice.

ACKNOWLEDGMENT

This material is based on research sponsored by AFRL/RW under agreement number FA8651-15-1-0001. The U.S. Government is authorized to reproduce and distribute reprints for Governmental purposes notwithstanding any copyright notation thereon.

The authors gratefully acknowledge the technical support of the IT department at Tennessee State University. More specifically, without the support of Mr. Ben Coleman the FLUENT server could not have been established and maintained.

DISCLAIMER

The views and conclusions contained herein are those of the authors and should not be interpreted as necessarily representing the official policies and endorsements, either expressed or implied, of AFRL/RW or the U.S. Government.

NOMENCLATURE

D cooling pipe inlet diameter (m)

DR coolant to mainstream density ratio = ρ_C / ρ_∞

IR coolant to mainstream momentum ratio = $\rho_C u_C^{\,2} / \rho_\infty u_\infty^{\,2}$

L coolant pipe length (m)

MR coolant to mainstream mass flux ratio = $\rho_C u_C / \rho_\infty u_\infty$

R_1 radius of curvature of the coolant pipe, if the center is to the right of coolant pipe (m). Note that the location of the center is chosen such that the pipe arc makes tangent at the pipe and mainstream flow intersection.

R_2 radius of curvature of the coolant pipe, if the center is to the left of coolant pipe (m).

Re local Reynolds number based on the distance from the mainstream inlet to coolant pipe exit

T_C coolant air temperature (K)

T_∞ mainstream flow air temperature (K)

T_w adiabatic wall temperature (K)

u_C coolant velocity (m/s)

u_∞ mainstream velocity (m/s)

VR coolant to mainstream velocity ratio = u_C / u_∞

X total length of the channel (m)

X_1 length of the channel from the center of coolant exit hole (m)

Y vertical distance between the wall of channel to the top surface (m)

Z width of the channel in spanwise direction (m)

Greek Symbols

β coolant pipe enlargement angle from inlet to exit (°)

ε film cooling effectiveness = $(T_\infty - T_w)/(T_\infty - T_C)$

$\bar{\varepsilon}$ average film cooling effectiveness as defined in Eq. (1)

ρ fluid density (kg/m^3)

REFERENCES

[1] Goldstein, R. J., Eckert, E. R. G., & Burggraf, F. Effects of hole geometry and density on three-dimensional film cooling. International Journal of Heat and Mass Transfer, 1974, 17(5), 595-607.

[2] Pedersen, D. R., Eckert, E. R. G., & Goldstein, R. J. Film cooling with large density differences between the mainstream and the secondary fluid measured by the heat-mass transfer analogy. Journal of Heat Transfer. 1977, 99(4), 620-627.

[3] Sinha, A. K., Bogard, D. G., & Crawford, M. E. Film-cooling effectiveness downstream of a single row of holes with variable density ratio. Journal of Turbomachinery. 1991, 113(3), 442-449.

[4] Baldauf, S. A., Scheurlen, M., Schulz, A., & Wittig, S. (2002, January). Correlation of film cooling effectiveness from thermographic measurements at engine like conditions. In ASME Turbo Expo 2002: Power for Land, Sea, and Air (pp. 149-162). American Society of Mechanical Engineers.

[5] Bunker, R. S. (2005). A review of shaped hole turbine film-cooling technology. Journal of heat transfer, 127(4), 441-453.

[6] Thole, K. A., Sinha, A., Bogard, D. G., & Crawford, M. E. (1992). Mean temperature measurements of jets with a crossflow for gas turbine film cooling application. Rotating Machinery Transport Phenomena, 69-85.
[7] Jessen, W., Schröder, W., & Klaas, M. (2007). Evolution of jets effusing from inclined holes into crossflow. International Journal of Heat and Fluid Flow, 28(6), 1312-1326.
[8] Kohli, A., & Bogard, D. G. (1997). Adiabatic effectiveness, thermal fields, and velocity fields for film cooling with large angle injection. Journal of Turbomachinery, 119(2), 352-358.
[9] Li, X. C., Subbuswamy, G., & Zhou, J. (2013). Performance of gas turbine film cooling with backward injection. Energy and Power Engineering, 5(04), 132-137.
[10] Zhang, X. Z., & Hassan, I. (2006). Film Cooling Effectiveness for an Advanced-Louver Cooling Scheme for Gas Turbines. Journal of Thermophysics and Heat Transfer, 20(4), 754-763.
[11] Fric, T. F., & Roshko, A. (1994). Vortical structure in the wake of a transverse jet. Journal of Fluid Mechanics, 279, 1-47.
[12] Khajehhasani, S. (2014) Numerical Modeling of Innovative Film Cooling Hole Schemes, Doctoral dissertation, Ryerson University, Canada.
[13] New, T. H., Lim, T. T., & Luo, S. C. (2003). Elliptic jets in cross-flow. Journal of fluid mechanics, 494, 119-140.
[14] Takahashi, H., Nuntadusit, C., Kimoto, H., Ishida, H., Ukai, T., & Takeishi, K. (2001). Characteristics of Various Film Cooling Jets Injected in a Conduit. Annals of the New York Academy of Sciences, 934(1), 345-352.
[15] Aga, V., Rose, M., and Abhari, R. S., 2008, "Experimental Flow Structure Investigation of Compound Angled Film Cooling", Journal of Turbomachinery, Vol. 130, No. 3, pp. 031005-1-8.
[16] Rigby, D. L., & Heidmann, J. D. (2008, January). Improved film cooling effectiveness by placing a vortex generator downstream of each hole. In ASME Turbo Expo 2008: Power for Land, Sea, and Air (pp. 1161-1174). American Society of Mechanical Engineers.
[17] Shangguan, Y., Wang, X., & Li, Y. (2016). Investigation on the mixing mechanism of single-jet film cooling with various blowing ratios based on hybrid thermal lattice Boltzmann method. International Journal of Heat and Mass Transfer, 97, 880-890.
[18] Haven, B. A., & Kurosaka, M. (1997). Kidney and anti-kidney vortices in crossflow jets. Journal of Fluid Mechanics, 352, 27-64.
[19] ANSYS Fluent Theory Guide (2015), Release 16.1, USA, ANSYS Inc.
[20] Sutherland, W. (1893). LII. The viscosity of gases and molecular force. The London, Edinburgh, and Dublin Philosophical Magazine and Journal of Science, 36(223), 507-531.
[21] Johnson, P. L., Shyam, V. & Hah, C. (2011) Reynolds-averaged Navier-Stokes solutions to flat plate film cooling scenarios. National Aeronautics and Space Administration. Glenn Research Center, NASA/TM—2011-217025.
[22] Son, P. N., Kim, J., & Ahn, E. Y. (2011). Effects of bell mouth geometries on the flow rate of centrifugal blowers. Journal of Mechanical Science and Technology, 25(9), 2267-2276.
[23] Mohamed, M. H., Ali, A. M., & Hafiz, A. A. (2015). CFD analysis for H-rotor Darrieus turbine as a low speed wind energy converter. Engineering Science and Technology, an International Journal, 18(1), 1-13.
[24] Balogh, M., Parente, A., & Benocci, C. (2012). RANS simulation of ABL flow over complex terrains applying an enhanced k-ε model and wall function formulation: Implementation and comparison for Fluent and OpenFOAM. Journal of Wind Engineering and Industrial Aerodynamics, 104, 360-368.
[25] AbdelGayed, H. M., Abdelghaffar, W. A., & El Shorbagy, K. (2013). Main flow characteristics in a lean premixed swirl stabilized gas turbine combustor–Numerical computations. American Journal of Scientific and Industrial Research, 123-136.